



# Chiral Perturbation Theory and Unitarization\*

Enrique Ruiz Arriola<sup>1\*\*</sup>, A. Gómez Nicola<sup>2</sup>, J. Nieves<sup>1</sup> and J. R. Peláez<sup>2</sup>

<sup>1</sup>Departamento de Física Moderna, Universidad de Granada, E-18071 Granada, Spain

<sup>2</sup>Departamento de Física Teórica Universidad Complutense, 28040 Madrid, Spain

**Abstract.** We review our recent work on unitarization and chiral perturbation theory both in the  $\pi\pi$  and the  $\pi N$  sectors. We pay particular attention to the Bethe-Salpeter and Inverse Amplitude unitarization methods and their recent applications to  $\pi\pi$  and  $\pi N$  scattering.

## 1 Introduction

Chiral Perturbation Theory (ChPT) is a practical and widely accepted effective field theory to deal with low energy processes in hadronic physics. [1–3]. The essential point stressed in this approach is that the low energy physics does not depend on the details of the short distance dynamics, but rather on some bulk properties effectively encoded in the low energy parameters. This point of view has been implicitly adopted in practice in everyday quantum physics; well separated energy and distance scales can be studied independently of each other. The effective field theory approach also makes such a natural idea into a workable and systematic computational scheme.

The great advantage of ChPT is that the expansion parameter can be clearly identified *a priori* (see e.g. Ref. [3]) when carrying out systematic calculations of mass splittings, form factors and scattering amplitudes. However, the connection to the underlying QCD dynamics becomes obscure since the problem is naturally formulated in terms of the relevant hadronic low energy degrees of freedom with no explicit reference to the fundamental quarks and gluons. In addition, in some cases (see below) a possible drawback is the lack of numerical convergence of such an expansion when confronted to experimental data, a problem that gets worse as the energy of the process increases. Recent analysis provide good examples of both rapid convergence and slow convergence in ChPT. In the  $\pi\pi$  sector the situation to two loops [4] seems to be very good for the scattering lengths. Here, the expansion parameter is  $m_\pi^2/(4\pi f_\pi)^2 = 0.01$  ( $m_\pi = 139.6\text{MeV}$  the physical mass of the charged pion) and the coefficients of the expansion are of order unity. For instance, to two loops (third order in the expansion parameter) the expansion of the s-wave of the isospin  $I = 0$  channel reads [5]

$$a_{00} m_\pi = \underbrace{0.156}_{\text{tree}} + \underbrace{0.043 \pm 0.003}_{\text{1 loop}} + \underbrace{0.015 \pm 0.003}_{\text{2 loops}} + \dots \quad (1)$$

\* Talk delivered by Enrique Ruiz Arriola

\*\* E-mail: earriola@ugr.es

where the theoretical errors are described in [5]. Thus the expansion up to two loops is both convergent  $a^{(n)} \gg a^{(n+1)}$  and predictive  $\Delta a^{(n)} \ll a^{(n+1)}$ ,  $\Delta a^{(n)} \ll a^{(n)}$ . The *prediction* of ChPT of s-wave scattering lengths  $a_{IJ}$  in the isospin  $I = 0$  and  $I = 2$  channels yields [5]

$$\begin{aligned} a_{00} m_\pi &= +0.214 \pm 0.005 \quad (\text{exp. } +0.26 \pm 0.05) \\ a_{20} m_\pi &= -0.420 \pm 0.010 \quad (\text{exp. } -0.28 \pm 0.12) \end{aligned} \quad (2)$$

The theoretical predictions for these observables are an order of magnitude more accurate than the corresponding experimental numbers. Note that in hadronic physics we are usually dealing with the opposite situation, confronting accurate measurements to inaccurate theoretical model calculations. On the contrary, for  $\pi N$  scattering, for ChPT in the heavy baryon formulation the expansion is less rapidly converging than in the  $\pi\pi$  case, since NLO corrections become comparable to the LO ones. For instance in the  $P_{33}$ -channel the expansion up to third order, after a fit to the threshold properties, reads [6]

$$a_{33}^1 m_\pi^3 = \underbrace{35.3}_{\text{1st order}} + \underbrace{47.95}_{\text{2nd order}} - \underbrace{1.49}_{\text{3rd order}} + \dots = 81.8 \pm 0.9 \quad (\text{exp. } 80.3 \pm 0.6) \quad (3)$$

Here first order means  $1/f_\pi^2$ , second order  $1/f_\pi^2 M_N$  and third order  $1/f_\pi^4$  and  $1/f_\pi^2 M_N^2$ . Despite these caveats, there is no doubt that the effective field theory approach provides a general framework where one can either verify or falsify, not only bulk properties of the underlying dynamics, but also the dynamics of all models sharing the same general symmetries of QCD.

Finally, let us remark that the perturbative nature of the chiral expansion makes the generation of pole singularities, either bound states or resonances, impossible from the very beginning unless they are already present at lowest order in the expansion. There are no bound states in the  $\pi\pi$  and  $\pi N$  systems, but the  $\rho$  and the  $\Delta$  resonances are outstanding features of these reactions dominating the corresponding cross sections at the C.M. energies  $\sqrt{s} = m_\rho = 770\text{MeV}$  and  $\sqrt{s} = m_\Delta = 1232\text{MeV}$  respectively.

## 2 The role played by unitarity

Exact Unitarity plays a crucial role in the description of resonances. However, ChPT only satisfies unitarity perturbatively. Nevertheless, there are many ways to restore exact unitarity out of perturbative information, i.e.: the K-matrix method Ref. [7], the Inverse Amplitude Method (IAM) Ref. [8,9], the Bethe-Salpeter Equation (BSE) Ref. [11,12], the N/D method Ref. [10], etc. ( See e.g. Ref. [13] for a recent review), which are closely related to one another.

Some of these Unitarization methods have been very successful describing experimental data in the intermediate energy region including the resonant behavior. Despite this success the main drawback is that this approach is not as systematic as standard ChPT, for instance in the estimation of the order of the neglected corrections. In this work we report on our most recent works related to

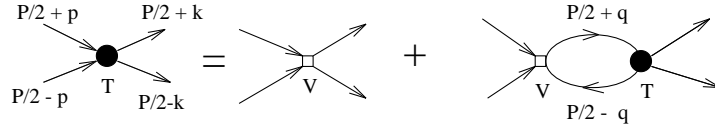


**Fig. 1.** Diagrammatic representation of the BSE equation. It is also sketched the used kinematics.

unitarization, both in the  $\pi\pi$  and  $\pi N$  sectors, where we have obtained intermediate energy *predictions* using the chiral parameters and their error bars obtained from standard ChPT applied at low energies. This means in practice transporting the possible correlations among the fitting parameters obtained from a fit where the phase shifts are assumed to be gauss-distributed in an uncorrelated way.

### 3 Results in the $\pi\pi$ sector

The ChPT expansion displays a very good convergence in the meson-meson sector. As a consequence the unitarization methods have been very successful in extending the ChPT applicability to higher energies. In particular, within a coupled channel IAM formalism, it has been possible to describe all the meson-meson scattering data, even the resonant behavior, below 1.2 GeV [9], but without including explicitly any resonance field. These works have already been extensively described in the literature and here we will concentrate in the most recent works of two of the authors on the  $\pi\pi$  sector, dealing with the Bethe-Salpeter equation, which has the nice advantage of allowing us to identify the diagrams which are resummed.

Indeed, any unitarization method performs, in some way or another, an infinite sum of perturbative contributions. At first sight, this may seem arbitrary, but some constraints have to be imposed on the unitarization method to comply with the spirit of the perturbative expansion we want to enforce. In the BSE approach the natural objects to be expanded are the *potential* and the *propagators*. The BSE as it has been used in Refs. [11,12] reads (See Fig. 1)

$$T_p^I(p, k) = V_p^I(p, k) + i \int \frac{d^4 q}{(2\pi)^4} T_p^I(q, k) \Delta(q_+) \Delta(q_-) V_p^I(p, q) \quad (4)$$

where  $q_{\pm} = (P/2 \pm q)$  and  $T_p^I(p, k)$  and  $V_p^I(p, k)$  are the total scattering amplitude<sup>1</sup> and potential for the channel with total isospin  $I = 0, 1, 2$ . and then the projection over each partial wave  $J$  in the CM frame,  $T_{IJ}(s)$ , is given by

$$T_{IJ}(s) = \frac{1}{2} \int_{-1}^{+1} P_J(\cos \theta) T_p^I(p, k) d(\cos \theta) = \frac{i8\pi s}{\lambda^{\frac{1}{2}}(s, m^2, m^2)} \left[ e^{2i\delta_{IJ}(s)} - 1 \right] \quad (5)$$

<sup>1</sup> The normalization of the amplitude  $T$  is determined by its relation with the differential cross section in the CM system of the two identical mesons and it is given by  $d\sigma/d\Omega = |T_p(p, k)|^2/64\pi^2 s$ , where  $s = P^2$ . The phase of the amplitude  $T$  is such that the optical theorem reads  $\text{Im}T_p(p, p) = -\sigma_{\text{tot}}(s^2 - 4s m^2)^{1/2}$ , with  $\sigma_{\text{tot}}$  the total cross section. The contribution to the amputated Feynman diagram is  $(-iT_p(p, k))$  in Fig. 1.

where  $\theta$  is the angle between  $\mathbf{p}$  and  $\mathbf{k}$  in the CM frame,  $P_j$  the Legendre polynomials and  $\lambda(x, y, z) = x^2 + y^2 + z^2 - 2xy - 2xz - 2yz$ . Notice that in our normalization the unitarity limit implies  $|T_{IJ}(s)| < 16\pi s/\lambda^{1/2}(s, m^2, m^2)$ .

The solution of the BSE at lowest order, i.e., taking the free propagators for the mesons and the potential as the tree level amplitude can be obtained after algebraic manipulations described in detail in Refs. [11,12], renormalization and matching to the Taylor expansion up to second order in  $s - 4m^2$  of the one loop chiral perturbation theory result. We only quote here the result for the  $\rho$  channel:

$$T_{11}^{-1}(s) = -\bar{I}_0(s) + \frac{1}{16\pi^2} \left[ 2(\bar{l}_2 - \bar{l}_1) + \frac{97}{60} \right] \quad (6)$$

$$+ \frac{1}{s - 4m^2} \left\{ \frac{m^2}{4\pi^2} \left[ 2(\bar{l}_2 - \bar{l}_1) + 3\bar{l}_4 - \frac{65}{24} \right] - 6f^2 \right\} \quad (7)$$

where the unitarity integral  $\bar{I}_0(s)$  reads

$$\bar{I}_0(s) \equiv I_0(s) - I_0(4m^2) = \frac{1}{(4\pi)^2} \sqrt{1 - \frac{4m^2}{s}} \log \frac{\sqrt{1 - \frac{4m^2}{s}} + 1}{\sqrt{1 - \frac{4m^2}{s}} - 1} \quad (8)$$

Here the complex phase of the argument of the log is taken in the interval  $[-\pi, \pi[$ . Similar expressions hold for the scalar-isoscalar ( $\sigma$ ) and the scalar-isotensor channels. Notice that in this, so-called *off-shell* scheme, the left hand cut is replaced at lowest order by a pole in the region  $s \ll 0$ . For the low energy coefficients  $\bar{l}_{1,2,3,4}$  we take the values

$$\text{set A: } \bar{l}_1 = -0.62 \pm 0.94, \bar{l}_2 = 6.28 \pm 0.48, \bar{l}_3 = 2.9 \pm 2.4, \bar{l}_4 = 4.4 \pm 0.3$$

$$\text{set B: } \bar{l}_1 = -1.7 \pm 1.0, \bar{l}_2 = 6.1 \pm 0.5, \bar{l}_3 = 2.9 \pm 2.4, \bar{l}_4 = 4.4 \pm 0.3 \quad (9)$$

In both sets  $\bar{l}_3$  and  $\bar{l}_4$  have been determined from the SU(3) mass formulae and the scalar radius as suggested in [1] and in [14], respectively. On the other hand the values of  $\bar{l}_{1,2}$  come from the analysis of Ref. [15] of the data on  $K_{14}$ -decays (set A) and from the combined study of  $K_{14}$ -decays and  $\pi\pi$  with some unitarization procedure (set B) performed in Ref. [16]. The results for the  $\rho$  channel are shown in Fig. 2.

As discussed in Ref. [12] it is also possible to take into account the left hand cut in the so-called *on-shell* scheme where it can be shown that after renormalization the on-shell unitarized amplitude acquires the following form

$$T_{IJ}(s)^{-1} + \bar{I}_0(s) - V_{IJ}(s)^{-1} = T_{IJ}(s_0)^{-1} + \bar{I}_0(s_0) - V_{IJ}(s_0)^{-1} = -C_{IJ} \quad (10)$$

where  $C_{IJ}$  should be a constant, independent of  $s$  and the subtraction point  $s_0$ , and chosen to have a well defined limit when  $m \rightarrow 0$  and  $1/f \rightarrow 0$ .  $V_{IJ}(s)$  is the *on-shell*-potential and has the important property of being real for  $0 < s < 16m^2$ , and presenting cuts in the four pion threshold and the left hand cut caused by the unitarity cuts in the  $t$  and  $u$  channels. The potential can be determined by matching the amplitude to the ChPT amplitude in a perturbative expansion. This method provides a way of generating a unitarized amplitude directly in terms of the low

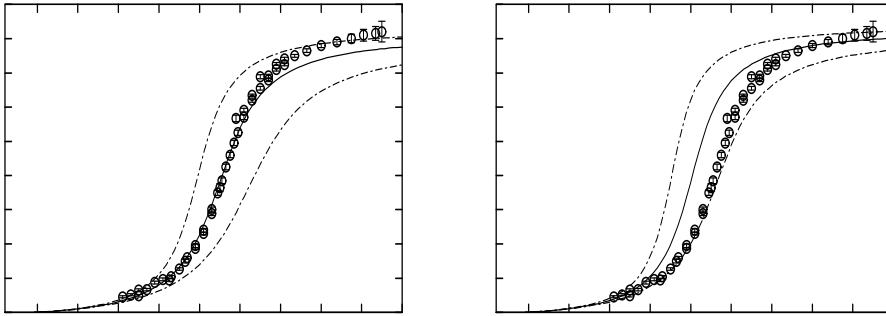


**Fig. 2.**  $I = J = 1$   $\pi\pi$  phase shifts as a function of the total CM energy  $\sqrt{s}$  for both sets of  $\bar{l}$ 's given in Eq. (9). Left (right) figures have been obtained with the set **A** (**B**) of parameters. Solid lines are the predictions of the off-shell BSE approach, at lowest order, for the different  $IJ$ -channels. Dashed lines are the 68% confidence limits. Circles stand for the experimental analysis of Refs. [17] and [18].

energy coefficients  $\bar{l}_{1,2,3,4}$  and their errors. In this *on-shell* scheme a successful description of both  $\pi\pi$  scattering data as well as the electromagnetic pion form factor, in agreement with Watson's theorem, becomes possible yielding a very accurate determination of some low energy parameters. The procedure to do this becomes a bit involved and we refer to Ref. [12] for further details. We should also say that the one-loop unitarized amplitudes generate the complete ChPT result and *some* of the two and higher loop results. The comparison of the generated two-loop contribution of threshold parameters with those obtained from the full two loop calculation is quantitatively satisfactory within uncertainties.

## 4 Results in the $\pi N$ sector

The methods and results found in the  $\pi\pi$  system are very encouraging, suggesting the extension to the  $\pi N$  system. However, ChPT does not work in the  $\pi N$  sector as nicely as it does in the  $\pi\pi$  sector. As we will see, the low convergence rate of the chiral expansion makes it difficult to match standard amplitudes to unitarized ones in a numerically sensible manner. After an initial attempt within the relativistic formulation [19], it was proposed to treat the baryon as a heavy particle well below the nucleon production threshold [20]. The resulting Heavy Baryon Chiral Perturbation Theory (HBChPT) provides a consistent framework for the one nucleon sector, particularly in  $\pi N$  scattering [6]. The proposal of Ref. [21] adopting the original relativistic formalism but with a clever renormalization scheme seems rather promising but unfortunately the phenomenological applications to  $\pi N$  scattering have not been worked out yet.

### 4.1 The IAM method in $\pi$ -N scattering

The inverse amplitude method (IAM) is a unitarization method where the inverse amplitude, and not the amplitude, is expanded, i.e., if we have the perturbative

expansion for the partial wave amplitude  $f(\omega)$ ,

$$f(\omega) = f_1(\omega) + f_2(\omega) + f_3(\omega) + \dots \quad (11)$$

with  $\omega = \sqrt{q^2 + m_\pi^2}$  and  $q$  the C.M. momentum, then one considers the expansion

$$\frac{1}{f(\omega)} = \frac{1}{f_1(\omega)} - \frac{f_2(\omega) + f_3(\omega)}{[f_1(\omega)]^2} + \frac{f_2(\omega)^2}{[f_1(\omega)]^3} + \dots \quad (12)$$

The IAM fulfills exact unitarity,  $\text{Im}f(\omega)^{-1} = -q$  and reproduces the perturbative expansion to the desired order.

This method has been applied for  $\pi N$  scattering [22] to unitarize the HBChPT results of Ref. [6] to third order. In this context, it is worth pointing out that the use of a similar unitarization method, together with very simple phenomenological models, was already successfully undertaken in the 70's (see [23] and references therein). Nonetheless, a systematic application within an effective Lagrangian approach was not carried out. In [22] the phase shifts for the partial waves up to the inelastic thresholds have been fitted, obtaining the right pole for the  $\Delta(1232)$  in the  $P_{33}$  channel. In that work, it has been pointed out that to get the best accuracy with data, one needs chiral parameters of unnatural size, very different from those of perturbative HBChPT. This is most likely related to the slow convergence rate of the expansion. However, it must be stressed that one can still reproduce the  $\Delta(1232)$  with second order parameters compatible with the hypothesis of resonance saturation [32]. In a subsequent work [24] we have proposed an improved IAM method based on a reordering of the HBChPT series. The encouraging results for the  $\Delta$ -channel have also been extended to the remaining low partial waves [25], as it can be seen in Fig. 3. In this case, the size of the chiral parameters is natural and the  $\chi^2$  per d.o.f is considerably better than the IAM applied to plain HBChPT.

## 4.2 BSE method and the $\Delta$ -resonance

Recently [26], we have used the BSE to HBChPT at lowest order in the chiral expansion and have looked at the  $P_{33}$  channel. We have found a dispersive solution which needs four subtraction constants,

$$f_{3/2,1}^{3/2}(\omega)^{-1} = -\frac{24\pi}{(\omega^2 - m^2)} \left\{ \frac{-f^2\omega}{2g_\lambda^2} + P(\omega) + (\omega^2 - m^2)\bar{J}_0(\omega)/6 \right\}$$

$$P(\omega) = m^3 \left( c_0 + c_1\left(\frac{\omega}{m} - 1\right) + c_2\left(\frac{\omega}{m} - 1\right)^2 + c_3\left(\frac{\omega}{m} - 1\right)^3 \right) \quad (13)$$

where the unitarity integral is given by

$$\bar{J}_0(\omega) \equiv J_0(\omega) - J_0(m) = -\frac{\sqrt{\omega^2 - m^2}}{4\pi^2} \left\{ \text{arcosh} \frac{\omega}{m} - i\pi \right\}; \quad \omega > m \quad (14)$$

The  $\chi^2$  fit yields the following numerical values for the parameters:

$$c_0^{\text{fit}} = 0.045 \pm 0.021, \quad c_1^{\text{fit}} = 0.29 \pm 0.08, \quad c_2^{\text{fit}} = -0.17 \pm 0.09, \quad c_3^{\text{fit}} = 0.16 \pm 0.03$$

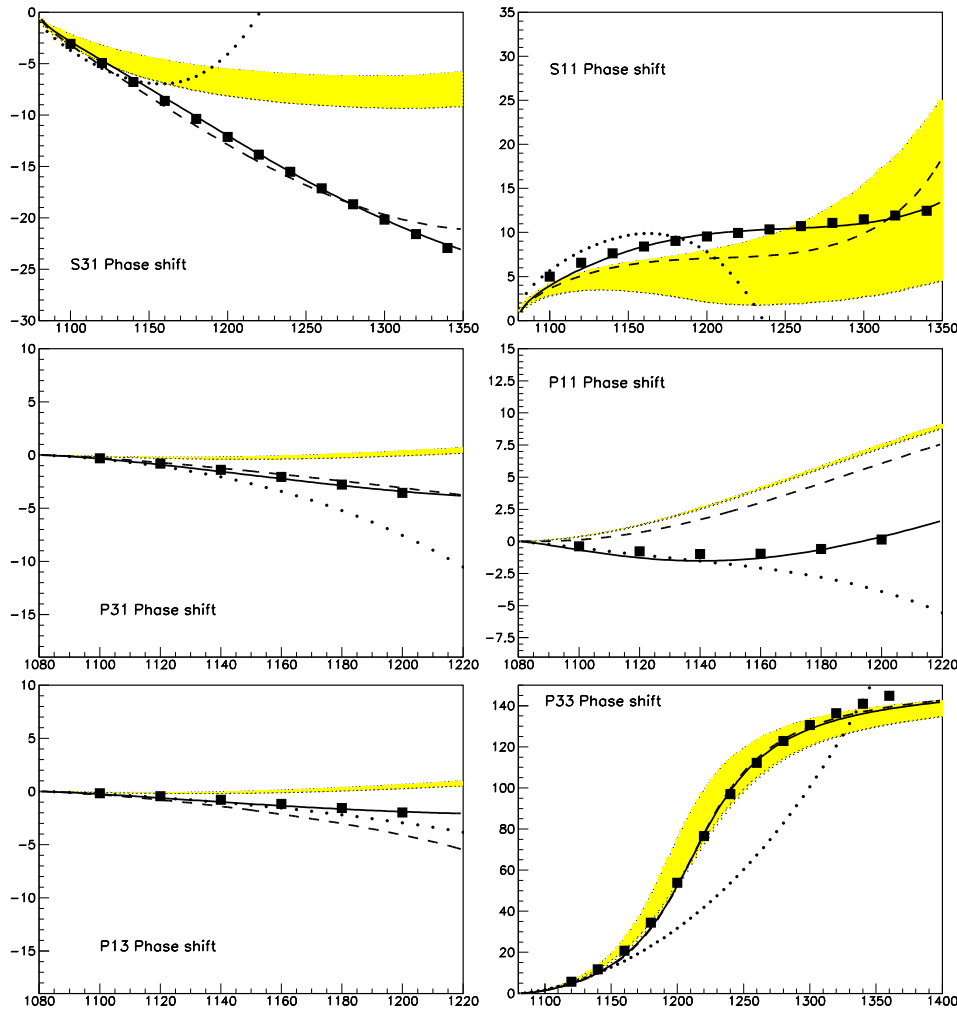


**Fig. 3.** Phase shifts in the IAM method as a function of the C.M. energy  $\sqrt{s}$ . The shaded area corresponds to the result of propagating the errors of the chiral parameters obtained from low-energy data (see Ref. [25]). This illustrates the uncertainties due to the choice of different parameter sets from the literature. The dotted line is the extrapolated HBChPT result. The continuous line is an unconstrained IAM fit to the data, whereas for the dashed line the fit has been constrained to the resonance saturation hypothesis.

with  $\chi^2/\text{d.o.f.} = 0.2$ . However, if we match the coefficients with those stemming from HBChPT we would get instead the following numerical values:

$$c_0^{\text{th}} = 0.001 \pm 0.003, \quad c_1^{\text{th}} = 0.038 \pm 0.006, \quad c_2^{\text{th}} = 0.064 \pm 0.005, \quad c_3^{\text{th}} = 0.036 \pm 0.002$$

The discrepancy is, again, attributed to the low convergence rate of the expansion. The results for the  $P_{33}$  phase shift both for the fit and the MonteCarlo propagated errors of the HBChPT matched amplitudes have been depicted in Fig. 4

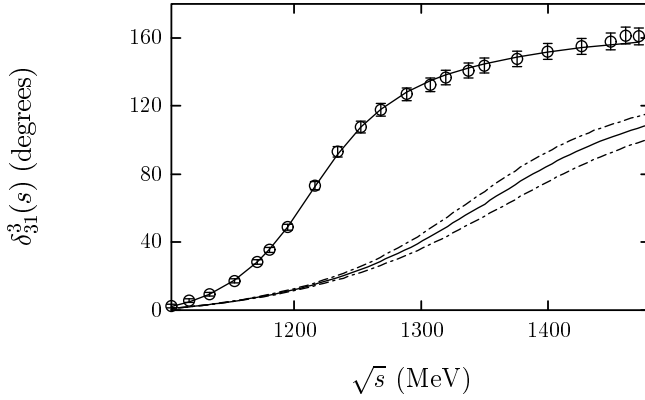


**Fig. 4.**  $P_{3,3}$  phase shifts as a function of the total CM energy  $\sqrt{s}$ . The upper solid line represents a  $\chi^2$ -fit of the parameters,  $c_{0,1,2,3}$  to the data of Ref. [31] (circles). Best fit parameters are denoted  $c_{0,1,2,3}^{\text{fit}}$  in the main text. The lower lines stand for the results obtained with the parameters deduced from HBChPT and denoted  $c_{0,1,2,3}^{\text{th}}$ . Central values lead to the solid line, whereas the errors on  $c_{0,1,2,3}^{\text{th}}$  lead to the dash-dotted lines.

### 4.3 $\pi N$ scattering and the $N^*(1535)$ resonance

One of the greatest advantages of both the IAM and the BSE methods is that the generalization to include coupled channels is rather straightforward. For the IAM case we refer to [9] for more details. As for the BSE, two of the authors [30] have dealt with the problem in the  $S_{11}$  channel, at  $\sqrt{s}$  up to 1800 GeV using the full relativistic, rather than the heavy baryon formulation used in Ref. [27] for the  $s$ -wave and extended in Ref. [28] to account for  $p$ -wave effects. For these energies there are four open channels, namely  $\pi N, \eta N, K\Sigma$  and  $K\Lambda$ , so that the BSE becomes a  $4 \times 4$  matrix equation for the  $I = 1/2, J = 1/2$  and  $L = 0$  partial wave. Additional complications arise due to the Dirac spinor structure of the nucleon, but the BSE can be analytically solved after using the above mentioned off-shell renormalization scheme. It turns out [30] that to lowest order in the potential and the propagators, one needs 12 unknown parameters, which should be used to fit experimental data. Several features make the fitting procedure a bit cumbersome. In the first place, there is no conventional analysis in the relativistic version of ChPT for this process and thus no clear constraints can be imposed on the unknown parameters. Secondly, the channel  $\pi N \rightarrow \pi\pi N$  is not included in our calculation. Therefore one should not expect perfect agreement with experiment, particularly in the elastic channel since it is known that 10 – 20% of the  $N^*$  resonance decay width goes into  $\pi\pi N$ . On the other hand, one cannot deduce from here how important is the  $\pi\pi N$  channel in the  $\eta$  production channel,  $\pi N \rightarrow \eta N$ . Actually, in Ref. [29] it has been suggested that the bulk of the process may be explained without appealing to the three body intermediate state  $\pi\pi N$ . The work of Ref. [29] would correspond in our nomenclature to the on-shell lowest order BSE approximation, which by our own experience describes well the bulk of the data. With the BSE we have provided a further improvement at low energies



by including higher order corrections. In the absence of a canonical low energy analysis it seems wiser to proceed using the off-shell renormalization scheme. In Fig. 5 we present a possible 12 parameter fit which accounts both for the elastic low and intermediate energy region and the lowest production channels. The failure to describe data around the  $N^*$  resonance is expected, since as we have already mentioned the  $\pi\pi N$  channel must be included. Our results seem to confirm the assumption made in Ref. [29] regarding the unimportance of the three body channel in describing the coupling of the  $N^*$  resonance to  $\eta N$ .

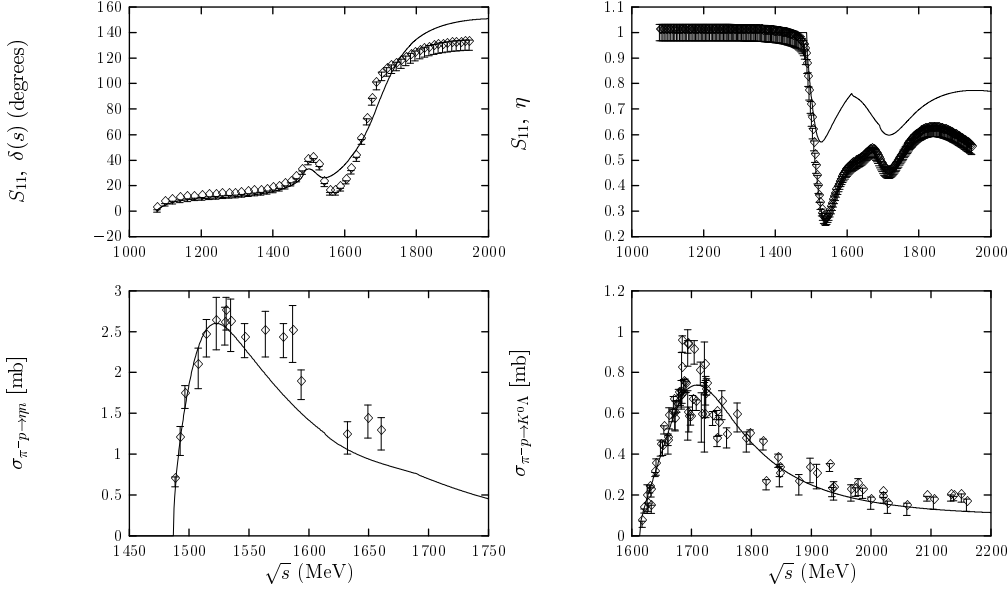


**Fig. 5.**  $\pi N$  scattering BSE results as a function of C.M. energy  $\sqrt{s}$ . Upper left figure:  $S_{11}$  phase shifts. Upper right figure: inelasticity in the  $\pi N$  channel. Lower left figure:  $\pi N \rightarrow \eta N$  cross section. Lower right figure:  $\pi N \rightarrow K\Lambda$  cross section. Data from Ref. [31]. (See Ref. [30] for further details.)

## 5 Conclusions and Outlook

The results presented here show the success and provide further support for unitarization methods complemented with standard chiral perturbation theory, particularly in the case when resonances are present. But unitarization by itself is not a guarantee of success; the unitarization method has to be carefully chosen so that it provides a systematic convergent and predictive expansion, as we have discussed above. In order to describe the data in the intermediate energy region the chiral parameters can then be obtained from

- Either a direct  $\chi^2$  fit of the order by order unitarized amplitude and the corresponding low energy parameters. The upper energy limit is determined by imposing an acceptable description  $\chi^2/\text{DOF} \sim 1$ .

- Or from a low energy determination of the low energy parameters with errors by performing a  $\chi^2$ -fit of the standard ChPT amplitude until  $\chi^2/\text{DOF} \sim 1$ , and subsequent MonteCarlo error propagation of the unitarized amplitude.

Differences in the low energy parameters within several methods should be compatible within errors, as long as the Chiral expansion has a good convergence. But, unfortunately this is not always the case. Clearly, the  $\pi\text{N}$  sector is not only more cumbersome theoretically than the  $\pi\pi$  sector but also more troublesome from a numerical point of view. Standard ChPT to a given order can be seen as a particular choice which sets higher order terms to zero in order to comply with exact crossing but breaking exact unitarity. The unitarization of a the ChPT amplitude is also another choice of higher order terms designed to reproduce exact unitarity but breaking exact crossing symmetry. Given our inability to write a closed analytic expression for an amplitude in a chiral expansion which simultaneously fulfills both exact crossing and unitarity we have preferred exact unitarity. This is justified a posteriori by the successful description of data in the intermediate energy region, which indeed suggests a larger convergence radius of the chiral expansion.

## Acknowledgments

This research was partially supported by DGES under contracts PB98-1367 and by the Junta de Andalucía FQM0225 as well as by DGICYT under contracts AEN97-1693 and PB98-0782.

## References

1. J. Gasser and H. Leutwyler, *Ann. of Phys.*, NY **158** (1984) 142.
2. H. Leutwyler, *Ann. of Phys.* NY **235** (1994) 165.
3. For reviews see e.g., A. Pich, *Rept. Prog. Phys.* **58** (1995) 563 and G. Ecker, *Prog. Part. Nucl. Phys.* **35** (1995) 1 for the meson sector, V. Bernard, N. Kaiser and U.-G. Meißner, *Int. J. Mod. Phys. E4* (1995) 193 for the baryon-meson system.
4. M. Knecht, B. Moussallam, J. Stern and N. H. Fuchs, *Nucl. Phys. B* **457** (1995) 513, *Nucl. Phys. B* **471** (1996) 445; J. Bijnens, G. Colangelo, G. Ecker J. Gasser and M. E. Sainio, *Phys. Lett. B* **374** (1996) 210, *Nucl. Phys. B* **508** (1997) 263.
5. J. Nieves and E. Ruiz Arriola, *Eur. Jour. Phys. A* **8** (2000) 377, G. Amoros, J. Bijnens and P. Talavera, *Nucl. Phys. B* **585** (2000) 293.
6. M. Mojzis, *Eur. Phys. Jour. C* **2** (1998) 181. N. Fettes, U.-G. Meißner and S. Steininger, *Nucl. Phys. A* **640** (1998) 199.
7. A. D. Martin and T.D. Spearman, *Elementary Particle Theory* (Wiley, New York ,1970) p. 348. S.N. Gupta, *Quantum Electrodynamics* (Gordon and Breach, New York,1981), p. 191.
8. T. N. Truong, *Phys. Rev. Lett.* **661** (1988) 2526; *Phys. Rev. Lett.* **67** (1991) 2260. A. Dobado, M.J. Herrero and T. N. Truong, *Phys. Lett.* **B235** (1990) 134. A. Dobado and J. R. Peláez, *Phys. Rev. D* **47** (1993) 4883; *Phys. Rev. D* **56** (1997) 3057.
9. J.A. Oller, E. Oset and J.R. Peláez, *Phys. Rev. Lett.* **80**(1998) 3452; *Phys. Rev. D* **59**(1999) 074001. F. Guerrero and J.A. Oller, *Nucl. Phys. B* **537** (1999) 3057.
10. J.A. Oller and E. Oset, *Phys. Rev. D* **60**: 074023,1999.

11. J. Nieves and E. Ruiz Arriola, Phys. Lett. B **455** (1999) 30.
12. J. Nieves and E. Ruiz Arriola, Nucl. Phys. A **679** (2000) 57.
13. J.A. Oller, E. Oset and A. Ramos, Prog. Part. Nucl. Phys. **45** (2000) 157.
14. J. Bijnens, G. Colangelo and P. Talavera, JHEP **9805** (1998) 014.
15. C. Riggenbach, J.F. Donoghue, J. Gasser, B.R. Holstein, Phys. Rev. D **43** (1991) 127.
16. J. Bijnens, G. Colangelo and J. Gasser, Nucl. Phys. B **427** (1994) 427.
17. S. D. Protopopescu *et. al.*, Phys. Rev. D **7** (1973) 1279.
18. P. Estabrooks and A. D. Martin, Nucl. Phys. B **79** (1974) 301.
19. J. Gasser, M.E. Sainio and A. Svarc, Nucl. Phys. B **307** (1988) 779.
20. E. Jenkins and A. V. Manohar, Phys. Lett. B **255** (1991) 558. V. Bernard, N. Kaiser, J. Kambor and U. -G. Meißner, Nucl. Phys. B **388** (1992) 315.
21. T. Becher and H. Leutwyler, Eur. Phys. Jour. C **9** (1999) 643.
22. A. Gómez Nicola and J.R. Peláez, Phys. Rev. D **62** (2000) 017502.
23. J.L. Basdevant, Fort. der Phys. **20** (1972) 283.
24. J. Nieves and E. Ruiz Arriola, hep-ph/0001013
25. A. Gómez Nicola, J. Nieves, J.R. Peláez and E. Ruiz Arriola, Phys. Lett. B **486** (2000) 77.
26. J. Nieves and E. Ruiz Arriola, Phys. Rev. D in print, hep-ph/0008034.
27. N. Kaiser, P.B. Siegel and W. Weise, Phys. Lett. B **362** (1995) 23.
28. J. Caro, N. Kaiser, S. Wetzel and W. Weise, Nucl. Phys. A **672** (2000) 249.
29. J.C. Nacher, A. Parreno, E. Oset, A. Ramos, M. Oka, Nucl. Phys. A **678** (2000) 187.
30. J. Nieves and E. Ruiz Arriola, work in progress.
31. R.A. Arndt, I.I. Strakovsky, R.L. Workman, and M.M. Pavan, Phys. Rev. C **52**, 2120 (1995). R.A. Arndt, *et. al.*, nucl-th/9807087. SAID online-program (Virginia Tech Partial-Wave Analysis Facility). Latest update, <http://said.phys.vt.edu>.
32. V. Bernard, N. Kaiser and U. -G. Meißner, Phys. Lett. B **309** (1993) 421; Phys. Rev. C **52** (1995) 2185; Phys. Lett. B **389** (1996) 144; Nucl. Phys. A **615** (1997) 483;